Streamlined spatial analysis of the brain tumor microenvironment and associated pathological states using multiplex immunohistochemistry

Introduction

Spatial studies of the tumor microenvironment are crucial for understanding the complex interactions between different cell types and how these interactions contribute to disease progression. The intricate complexity of the brain tumor microenvironment presents significant challenges and opportunities for scientific exploration. Understanding the spatial relationships and molecular dynamics within this environment is crucial for advancing research strategies. Leveraging advanced imaging technologies like the Invitrogen™ EVOS™ S1000 Spatial Imaging System alongside innovative labeling solutions, researchers can gain exceptional insights into spatial localization of proteins and ribonucleic acids not readily available with conventional microscopy.

Traditional immunohistochemistry (IHC) using primary and secondary antibodies has many disadvantages including longer assay times and additional steps, as well as higher risk of non-specific binding, which can lead to increased background staining and reduced signal-to-noise ratio. Additionally, limited species availability makes it challenging to simultaneously stain tissue with more than four primary-secondary antibody pairs. Multiplex staining with primary antibody conjugates bypasses these challenges. With Invitrogen™ IHC-verified primary antibody conjugates, staining can be completed in a single incubation step as short as one hour, delivering significant reduction in sample preparation time and improved images.

When commercially available antibody conjugates are not a feasible option, Invitrogen™ ReadyLabel™ Antibody Labeling Kits help bridge the gap of conjugate availability. These kits feature spectrally diverse Invitrogen™ Alexa Fluor™ and Alexa Fluor™ Plus dyes designed for spatial imaging. Additionally, these kits provide a built-in antibody purification system, enabling direct antibody labeling in BSA or other protein stabilizers for a more streamlined workflow.

Designed to be spectrally compatible and interchangeable, these two labeling solutions are demonstrated to be capable of combining to design a 9-plex panel to investigate the brain tumor microenvironment. When paired with the advanced spectral detection capabilities of the EVOS S1000 Spatial Imaging System and Indica Labs HALO® Image Analysis software, this panel provides characterization of healthy and pathological structures, offering a deeper understanding of brain tumor pathology.

Materials & Methods

Three brain-specific antibodies were conjugated with the 20 µg ReadyLabel Antibody Labeling Kits following the standard protocol.

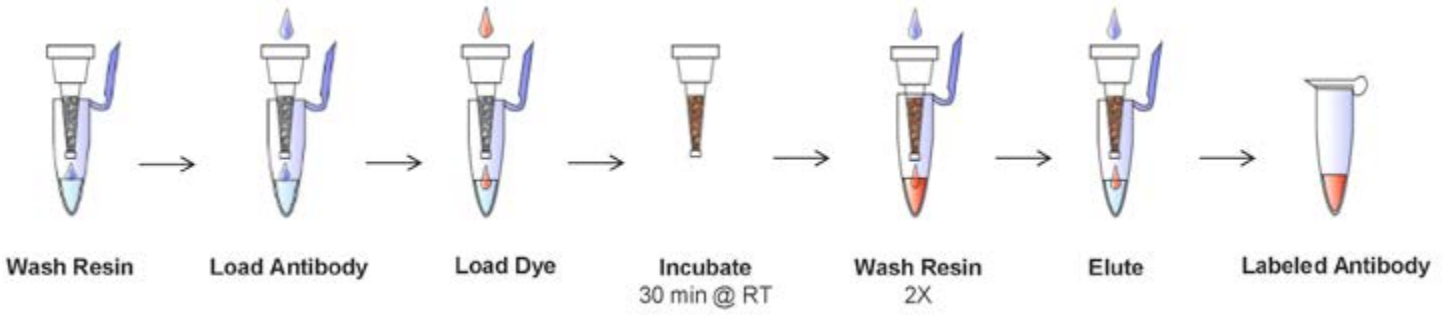

Figure 1. Workflow for labeling unconjugated antibodies using the ReadyLabel Antibody Labeling Kits.

Immunohistochemical analysis was performed on formalin-fixed paraffin-embedded (FFPE) healthy human frontal lobe tissue sample from a 73-year-old male, as well as human mixed glioma (astrocytoma and oligodendroglioma) brain tumor tissue sample from the frontal lobe of a 41-year-old male. To expose the target proteins, heat-induced epitope retrieval was performed on de-paraffinized sections using BOND™ Epitope Retrieval Solution 2 (pH 9) (Leica Biosystems) for 20 minutes, followed by a 5-minute cooldown and a 5-minute wash with ddH_2O. Tissues were permeabilized with 0.1% Triton™ X-100 in 1X PBS for 30 minutes and blocked with 3% BSA/5% NGS in 1X PBS for 1 hour at room temperature. Following removal of the blocking solution, tissues were probed overnight at 4°C in a humidified chamber with the antibody conjugates shown in the table below.

Table 1

Antibody (Clone)	Fluorophore	Cellular target	Staining concentration	Conjugate source	Expected expression
Vimentin (V9)	Alexa Fluor 420	Endothelial cells, astrocytes	5 µg/mL	Validated	Upregulation
GFAP (GA5)	Alexa Fluor 488	Astrocytes	3 µg/mL	Validated	Upregulation, morphological changes
Synaptophysin (EP10)	Alexa Fluor 514	Presynaptic vesicles	20 µg/mL	ReadyLabel	Variable by tumor origin
PCNA (PC10)	Alexa Fluor Plus 555	Proliferating cells	20 µg/mL	Validated	Possible upregulation
MAP2 (M13)	Alexa Fluor 594	Neurons	15 µg/mL	ReadyLabel	Variable by tumor type
Olig2 (OLIG2/7366R)	Alexa Fluor 647	Oligodendrocytes	20 µg/mL	ReadyLabel	Variable by tumor classification
p53 (DO-7)	Alexa Fluor 700	Tumor suppressor protein	10 µg/mL	Validated	Downregulation
CD68 (KP1)	Alexa Fluor Plus 750	Microglia	10 µg/mL	Validated	Possible upregulation

Tissue samples were washed three times in 1X PBS and panel tissues were stained with Thermo Scientific™ DAPI Nucleic Acid Stain diluted to 1 µg/mL in 1X PBS for 5 minutes at room temperature, then washed twice in 1X PBS. Tissues were mounted with Invitrogen™ ProLong™ Glass Antifade Mountant and cured overnight at room temperature. Single-color controls and panel images were captured and stitched on the EVOS S1000 Spatial Imaging System at 20X magnification. Spectral unmixing was performed in the S1000 software after the creation of a protocol utilizing single color control samples. Analyses of the multiplex stitched images were performed using Indica Labs HALO® software (v 4.0.5107.207). 12,058 cells (255 cells/mm^2) were identified in the frontal lobe tissue section and 88,124 cells (749 cells/mm^2) were identified in the glioma tissue section using the Indica Labs Halo® Highplex FL module (version 4.2.14) and the HALO AI Nuclei Seg V2-FL classifier.

Results

The nine-plex panel (including DAPI) used to stain the frontal lobe of human brain tissue samples was designed to identify cellular types and morphology. The entire antibody labeling and staining workflow required about three hours for 22 tissue samples, making this method highly efficient for multiplex IHC. The selection of markers was guided by their relevance to key cellular populations and tumor-associated changes. Glial Fibrillary Acidic Protein (GFAP) and Vimentin were included to identify astrocytic density and morphology, which are altered in astrocytoma. Similarly, Oligodendrocyte Transcription Factor 2 (Olig2) was selected to identify cellular density of oligodendrocytes. Proliferating Cell Nuclear Antigen (PCNA) was included because cellular proliferation may be expected in tumorous tissue. Synaptophysin was chosen to assess synapses, which may appear normal in astrocytoma or oligodendroglioma, while Microtubule-Associated Protein-2 (MAP2) primarily marks neuronal cells, but may sometimes be observed in oligodendrocytic and astrocytic cell populations. CD68 was included to identify tumor-associated microglia and the immune microenvironment, while p53 was used to evaluate tumor suppressor activity, as its loss or mutation is common in gliomas. This panel enabled spatial analysis of critical molecular signatures, revealing distinct expression patterns that differentiate healthy brain tissue from gliomas.

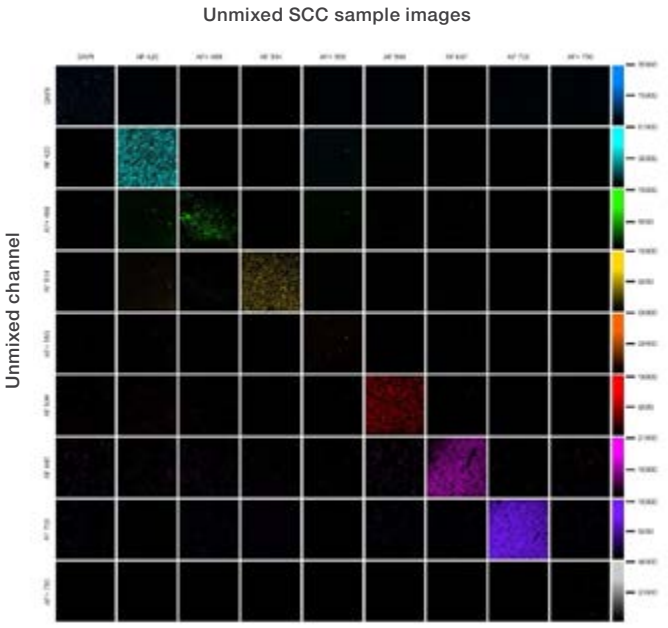

Figure 2. Visualization of the spectrally unmixed images acquired with the EVOS S1000 for single color control samples (in each column) in each of the primary channels (in every row). This information is shown in the quality metrics report generated by the instrument as part of the unmixing matrix creation.

Differences in cellular morphology and distribution were observed in the tissue sample, as compared to a healthy tissue sample. The tumor tissue exhibited an overall 294% increase in cell density per mm^2. Colocalization of Vimentin with GFAP significantly increased (~53%), compared with <1% colocalization in the healthy tissue sample. GFAP appeared as a dense mass in the tumor tissue and exhibited an altered morphology and a 700% increase in positive cells per mm^2. The abundance of synapses as marked by Synaptophysin appeared to be relatively unchanged; however, the morphology appeared to be disrupted. MAP2 exhibited an altered morphology and a 42% decrease in the percentage of cells in the tumor tissue. A 4.6 fold decrease in the percentage of cells positive for p53 was observed in the tumor tissue, as compared to healthy tissue sample. Upregulated expression of microglia was observed in the tumor tissue sample, as exhibited by a 16-fold increase in CD68-positive cells. Finally, an increase in abundance of Olig2 in the glioma (vs healthy) tissue was also registered, albeit only qualitatively.

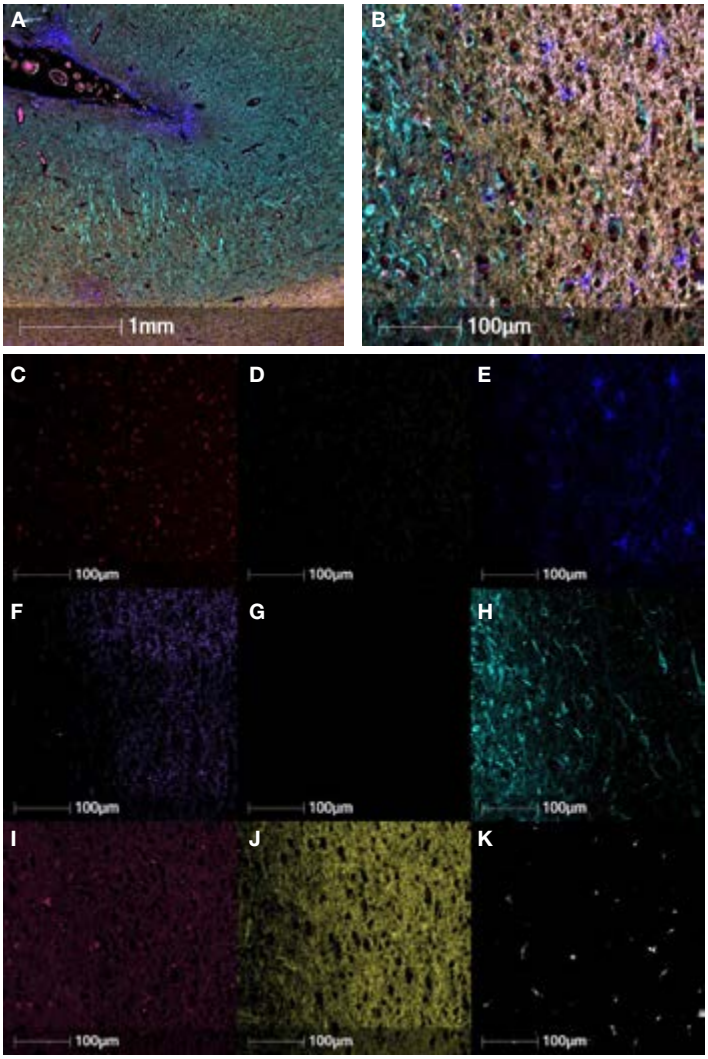

Figure 3. (a) Healthy human frontal lobe tissue sample was stained with a panel of primary antibody conjugates. Tissue was imaged and unmixed at 20X on the EVOS S1000 Spatial Imaging System. Image brightness and contrast were adjusted, color channels were merged, and cellular analysis was automated using HALO image analysis software. (b) Region of Interest (ROI) gathered from the full tissue sample scan shown in (a) demonstrated cellular morphology and distribution in healthy tissue. The healthy tissue staining pattern is further demonstrated in insets (c) DAPI nuclear stain (red), (d) Vimentin, marking endothelial cells and some astrocytes (green), (e) astrocytic marker GFAP (blue), (f) synaptic marker synaptophysin (purple), (g) PCNA (orange), (h) neuronal marker MAP2 (cyan), (i) Olig2 (magenta), (j) tumor suppressor protein p53 (yellow), and (k) microglia marker CD68 (white).

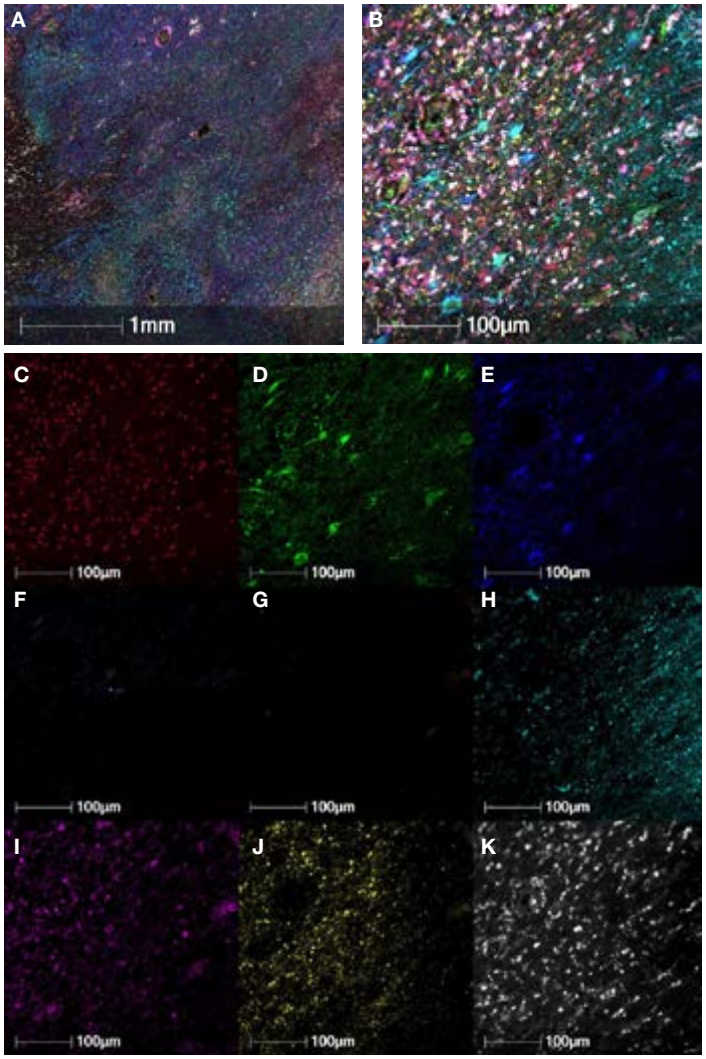

Figure 4. (a) Tumor tissue sample from the right frontal lobe of a 41-year-old male stained with a panel of primary antibody conjugates. Tissue sample was imaged and unmixed at 20X on the EVOS S1000 Spatial Imaging System. Image brightness and contrast were adjusted, and cellular analysis was automated using HALO image analysis software. (b) ROI gathered from the full tissue scan shown in (a) demonstrated differences in cellular morphology and distribution, as compared to a healthy tissue sample, Figure 3. Insets: (c) DAPI (red), (d) Vimentin (green), (e) GFAP (blue), (f) Synaptophysin (yellow), (g) PCNA (orange), (h) MAP2 (cyan), (i) Olig2 (magenta), (j) p53 (purple), (k) CD68 (white).

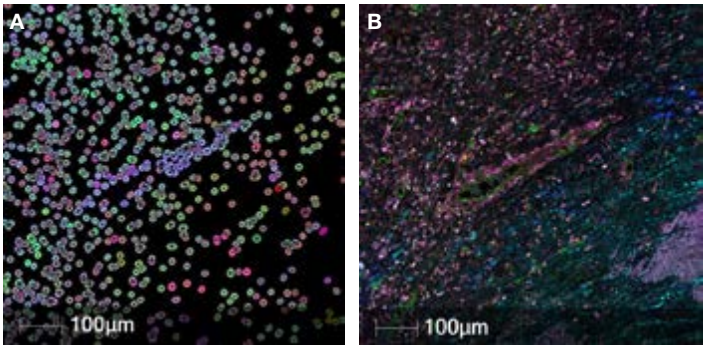

Figure 5. (a) Visual representation of HALO cellular segmentation and detection analysis showing an ROI in the panel-stained brain tumor tissue sample. Cell types are indicated by color, where the color is matched to the images in Figures 3 and 4; cells positive for multiple markers are displayed as mixed colors. (b) The original unmixed and tiled fluorescent ROI of brain tumor tissue sample depicted in the cellular analysis shown in a.

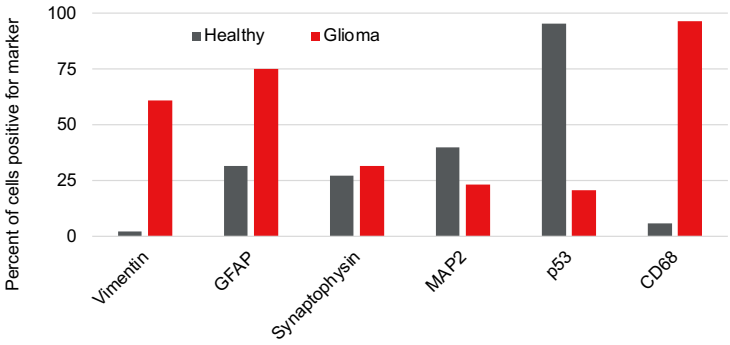

Figure 6. The percentage of cells determined to be positive for each of several markers, as determined by HALO analysis software.

Conclusions

Cellular analyses of similar brain regions in healthy versus tumor tissue samples show dramatic differences in the distribution and morphology of astrocytes and oligodendrocytes as well as overall cell density. Differences in neuronal cells were relatively minimal. The overall cellular density of the tumor tissue sample was three times that of the healthy tissue sample. Significant upregulation was observed in astrocytes and microglia, while tumor suppressor protein p53 exhibited significant downregulation. While cell count analysis was not performed for oligodendrocytes, visual inspection confirms upregulation in the tumor tissue sample. These results are consistent with expectations based on the literature.

The availability of IHC-validated primary antibody conjugates paired with the ease of ReadyLabel Antibody Labeling for specific targets allowed IHC staining of this 9-plex panel on two tissue types, in less than 24 hours and with minimal hands-on lab time, including antibody conjugation. Creation of the unmixing protocol and image capture, stitching, and integrated unmixing using the EVOS S1000 Spatial Imaging System was efficient; the instrument and software were intuitive and user-friendly. Finally, Indica Labs HALO Image Analysis software allowed adjustments and merging of the 9-plex panels, along with easy generation of figures, including the tiled single-channel images shown in Figures 3 and 4. The software's segmentation AI capabilities allowed the counting and analysis of entire tissue samples (tens of thousands of cells) in a matter of a few hours, including time to learn the software. The combination of these tools offers an overall streamlined workflow as compared to traditional IHC, imaging, and analysis.

Our study highlights the efficiency and effectiveness of primary conjugated antibodies, which streamline the labeling and staining workflow. This efficiency does not compromise the quality of the results; instead, it facilitates spatial analysis of complex tissue structures. The distinct expression patterns observed in glioma samples underscore the utility of this approach in differentiating between healthy and diseased states. The combination of tools used within this study, which enhances our ability to visualize and characterize the complex cellular and molecular interactions within brain tumors, is poised to accelerate our understanding of cancer biology.

References

Ang, L.C., *et al.* Proliferating cell nuclear antigen expression in the survival of astrocytoma patients. *Canadian J. of Neuro. Sciences*. 1994; 21(4): 306-310.

Blümcke, I., *et al.* Distinct expression pattern of microtubule-associate protein-2 in human oligodendrogliomas and glial precursor cells. *J. Neuropathol & Exp. Neurol.* 2001 Oct; 60(10): 984-993.

Hewedi, I.H., *et al.* Perspectives on the immunologic microenvironment of astrocytomas. *Cancer Manag. Res.* 2013 Aug; 5:293-299.

Kim, SI, *et al.* Revisiting vimentin: a negative surrogate marker of molecularly defined oligodendroglioma in adult type diffuse glioma. *Brain Tumor Pathol.* 2021 Aug; 38:271-282.

Kros, J.M., *et al*. Expression of p53 in oligodendrogliomas. *J. Pathol.* 1993 Dec; 171(4): 285-290.

Li, H., *et al.* New insights into the roles of p53 in central nervous system diseases. *Int. J. of Neuropsychopharmacol.* 2023 Jul; 26(7): 465-473.

Ligon, K.L., *et al.* The oligodendroglial lineage marker Olig2 is universally expressed in diffuse gliomas. *J. Neuropathol & Exp. Neurol.* 2004 May; 63(5): 499-509.

Nowicki, M.O., *et al.* Proteomic analysis implicates vimentin in glioblastoma cell migration. *Cancers (Basel).* 2019 Apr; 11(4):466.

Quinn, B. Synaptophysin staining in normal brain: importance for diagnosis of ganglioglioma. *Am. J. of Surg. Path.* 1998 May; 22(5): 550-556.

Van Bodegraven, E.J., *et al.* Importance of GFAP isoform-specific analyses in astrocytoma. *Glia.* 2019 Aug; 67(8): 1417-1433.

Wesseling, P., van den Bent, M., & Perry, A. Oligodendroglioma: pathology, molecular mechanisms and markers. *Acta Neuropathol.* 2015 May; 129: 809-827.

Zhang, J., *et al.* Role of CD68 in tumor immunity and prognosis prediction in pan-cancer. *Nature Sci. Reports*. 2022 May; 12: 7844

Ordering information

Product	Catalog Number
IHC-verified antibody conjugates	
Vimentin Monoclonal Antibody (V9), Alexa Fluor 420	758-9897-82
GFAP Monoclonal Antibody (GA5), Alexa Fluor 488	53-9892-82
PCNA Monoclonal Antibody (PC10), Alexa Fluor Plus 555	754-9910-82
p53 Monoclonal Antibody (DO-7), Alexa Fluor 700	56-8002-94
CD68 Monoclonal Antibody (KP1), Alexa Fluor Plus 750	757-0688-82
Antibody labeling kits	
ReadyLabel Alexa Fluor 514 Antibody Labeling Kit	R10720
ReadyLabel Alexa Fluor 594 Antibody Labeling Kit	R10722
ReadyLabel Alexa Fluor 647 Antibody Labeling Kit	R10710
Primary unconjugated antibodies	
Synaptophysin (EP10)	14-6525-82
MAP2 (M13)	13-1500
Olig2 (OLIG2/7366R)	10215-RBM6-P1ABX
Other reagents	
DAPI Nucleic Acid Stain	62248
ProLong Glass Antifade Mountant	P36980
1X PBS, pH 7.4	10010049
EVOS S1000 Spatial Imaging System	AMFS1000
FFPE Human Frontal Lobe Tissue	Biochain T2234051
FFPE Human Mixed Glioma Tissue	Biochain T2235035-12

Learn more at **thermofisher.com/spatial-biology**